ZOOLOGICAL SCIENCE **32**: 596–604 (2015)

Tubulanus tamias sp. nov. (Nemertea: Palaeonemertea) with Two Different Types of Epidermal Eyes

Hiroshi Kajihara[1]*, Keiichi Kakui[1], Hiroshi Yamasaki[2], and Shimpei F. Hiruta[1]

[1]*Faculty of Science, Hokkaido University, Sapporo 060-0810, Japan*
[2]*Faculty of Science, University of the Ryukyus, Senbaru 1, Nishihara, Nakagami, Okinawa 903-0213, Japan*

Based on specimens collected subtidally (~10 m in depth) in Tomioka Bay, Japan, we describe the palaeonemertean *Tubulanus tamias* sp. nov., which differs from all its congeners in body coloration. In molecular phylogenetic analyses based on partial sequences of the nuclear 18S and 28S rRNA genes and histone H3, as well as the mitochondrial 16S rRNA and cytochrome *c* oxidase subunit I genes, among selected palaeonemerteans, *T. tamias* nested with part of the congeners in *Tubulanus*, while the genus as currently diagnosed appears to be non-monophyletic. Molecular cloning detected polymorphism in 28S rDNA sequences in a single individual of *T. tamias*, indicating incomplete concerted evolution of multiple copies. *Tubulanus tamias* is peculiar among tubulanids in having 9–10 pigment-cup eyes in the epidermis on either side of the head anterior to the cerebral sensory organs, and remarkably there are two types of eyes. The anterior 8–9 pairs of eyes, becoming larger from anterior to posterior, are completely embedded in the epidermis and proximally abutting the basement membrane; each pigment cup contains bundle of up to seven, rod-shaped structure that resemble a rhabdomeric photoreceptor cell. In contrast, the posterior-most pair of eyes, larger than most of the anterior ones, have an optical cavity filled with long cilia and opening to the exterior, thus appearing to have ciliary-type photoreceptor cells. The size and arrangement of the eyes indicate that the posterior-most pair of eyes are the remnant of the larval (or juvenile) eyes.

Key words: ribbon worm, Anopla, Tubulanidae, ocellus, marine invertebrate, Amakusa

INTRODUCTION

The palaeonemertean genus *Tubulanus* Renier, 1804 contains 34 valid species of marine, benthic forms (Fernández-Álvarez and Anadón, 2013; Gibson, 2014) that often have characteristic body coloration. Four species have been reported from Japanese waters: *T. capistratus* (Coe, 1901); *T. ezoensis* Yamaoka, 1940; *T. punctatus* (Takakura, 1898); and *T. roretzi* Senz, 1997. *Tubulanus lucidus* Iwata, 1952 has a mid-dorsal blood vessel, a character uncommon in Palaeonemertea s.str. (i.e., non-hubrechtellid forms that do not produce a pilidium larva); this species appears to belong to *Hubrechtella* or a related genus, rather than to *Tubulanus* (Kajihara, 2007).

During a faunal survey around Tomioka, Kyushu, Japan, we collected specimens of an undescribed species of *Tubulanus* having eyes. Of ~110 described species in Palaeonemertea s.str., this is the seventh species known to have definitive eyes. The main aims of this paper are (1) to describe the species from Tomioka as new to science, and (2) to infer the phylogenetic position of the species among other select palaeonemerteans for which sequences are available in GenBank. We discuss the possible developmental pattern of eyes in this species based on the observation of adult morphology. We sequenced part of the 16S, 18S, and 28S rDNA, as well as histone H3 and cytochrome *c* oxidase subunit I (COI) genes to confirm the generic placement, and in the course of this analysis discovered polymorphism of 28S rDNA sequences, which we also report here.

* Corresponding author. Tel. : +81-11-706-2755;
Fax : +81-11-706-4851;
E-mail: kazi@mail.sci.hokudai.ac.jp
Supplemental material for this article is available online.
doi:10.2108/zs140250

MATERIALS AND METHODS

Sampling and morphological observation

Three anterior fragments of nemerteans were obtained with a Smith-McIntire grab sampler on 25 November 2009 from muddy-sand sediment at 9.7 m depth at Tomioka Bay (32°31′42″N, 130°02′15″E), Kyushu, Japan, by the research boat *Seriola* of the Amakusa Marine Biological Laboratory, Kyushu University. The fragments were anaesthetized in a $MgCl_2$ solution isotonic to seawater; the posterior portions of the two of the fragments were fixed and preserved in 100% EtOH for DNA extraction. Fragments for histological observation were fixed in Bouin's solution for 24 h and then preserved in 70% EtOH. They were dehydrated in 100% EtOH, cleared in xylene, embedded in paraffin wax (melting point 56–57°C), and sectioned at 9 or 14 μm thickness. Sections were stained using the Mallory trichrome method (Gibson, 1994). Terminology for morphological characters is based largely on Sundberg et al. (2009); the character matrix is available online as a supplementary file (Table S1). The ratio of the epidermal thickness to the body diameter in the brain and intestinal regions was calculated as the index *E* (*b*) and *E* (*i*), respectively, following Kajihara (2006). Sections are deposited in the Hokkaido University Museum, Sapporo, Japan (ZIHU).

DNA extraction, PCR amplification, sequencing

Total genomic DNA was extracted from the holotype and one of the paratypes of the new species by using a DNeasy Tissue Kit (Qiagen, Tokyo, Japan). PCR amplifications for 16S rRNA, 18S rRNA, H3, and COI genes were performed following the procedure described in Andrade et al. (2012). For 28S rRNA gene, about 2500 bp (corresponding roughly to the D1 through D7 regions; Gillespie et al., 2006), was PCR-amplified using the primer pair 28S-01 (Kim et al., 2000) and 28S_3KR (Yamasaki et al., 2013) (Table 1) with a thermal cycler (iCycler, Bio-Rad Laboratories, Tokyo, Japan). PCR cycling conditions were 95°C for 1 min; 35 cycles of 95°C for 30 sec, 50°C for 30 sec, and 72°C for 3 min; and 72°C for 7 min. Cycle sequencing was carried out with an ABI BigDye Terminator version 3.1 Cycle Sequencing Kit using the primers listed in Table 1. As we detected two apparently polymorphic sites (one near the D2 region, the other between D7a and D7b), we designed specific primers (N28_06F, N28_15F, and N28_19R, Table 1) that bind sites outside the polymorphic sites. PCR products that included the two polymorphic sites were inserted in pGEM-T Easy Vector (Promega, Tokyo, Japan) and transformed into competent DH5α *Escherichia coli* cells. Inserts were amplified from individual colonies by PCR using the M13 primer (Promega, Tokyo, Japan) to provide template for DNA sequencing. The sequences obtained have been deposited in the DNA Data Bank of Japan (DDBJ) under accession numbers AB854621–AB854624 and LC042091–LC042094 (Tables 2, 3). For comparison, a 2419-base fragment of the 28S rDNA gene was sequenced from *Tubulanus ezoensis* (voucher specimen, ZIHU 4458; DDBJ AB854620; Table 2) collected on 11 July 2010 at Daikoku-jima, Akkeshi, Hokkaido, Japan.

Phylogenetic analysis

To assess the phylogenetic position of the new species, a maximum-likelihood (ML) analysis and Bayesian inference (BI) were carried out using sequences from 20 palaeonemertean species (including the new species and *T. ezoensis*), as well as two brachiopod species as outgroups, which are available in public databases (Table 2). Sequences were aligned gene by gene by using MUSCLE (Edgar, 2004) implemented in MEGA ver. 5.2.2 (Tamura et al., 2011) with default settings. Alignment-ambiguous regions were removed by using BMGE ver. 1.1 (Criscuolo and Gribaldo, 2010); the 16S, 18S, and 28S alignments were processed with the "-t DNA" option, while H3 and COI were processed with the "-t CODON" option. The lengths of the resulting sequence alignments were 1644 nt (18S), 1112 nt (28S), 327 nt (H3), 357 nt (16S), and

Table 1. List of primers used in this study.

Name	Direction	Sequence (5′–3′)	Source
28S-01	forward	GACTACCCCCTGAATTTAAGCAT	Kim et al. (2000)
28SR-01	reverse	GACTCCTTGGTCCGTGTTTCAAG	Kim et al. (2000)
28Sf	forward	TGGGACCCGAAAGATGGTG	Luan et al. (2005)
28S_15R	reverse	CGATTAGTCTTTCGCCCCTA	Yamasaki et al. (2013)
28S_16F	forward	CATCCGGTAAAGCGAATGAT	present study
28S_2KF	forward	TTGGAATCCGCTAAGGAGTG	Yamasaki et al. (2013)
28S_3KR	reverse	CCAATCCTTTTCCCGAAGTT	Yamasaki et al. (2013)
N28_06F	forward	CGATCGAGGAAGACCGTAAATC	present study
N28_15F	forward	GGACGAAGCCAGAGGAAACTC	present study
N28_19R	reverse	CTTTTATGGTGTCCGATCAGC	present study

Table 2. Taxa included in the phylogenetic analysis, with GenBank accession numbers and source.

Taxa	18S	28S	H3	16S	COI	Source
Ingroup						
Callinera grandis Bergendal, 1903	JF293067	HQ856881	JF277709	JF277570	HQ848626	Andrade et al. (2012)
Carinina ochracea Sundberg et al., 2009	JF293050	HQ856896	JF277753	JF277631	HQ848627	Andrade et al. (2012)
Carinina plecta Kajihara, 2006	EU495307	—	—	—	EU489493	Sundberg et al. (2009)
Carinoma hamanako Kajihara et al., 2011	JF293047	HQ856863	JF277714	JF277600	HQ848628	Andrade et al. (2012)
Carinoma mutabile Griffin, 1898	—	AJ436887	AJ436985	AJ436832	—	Thollesson and Norenburg (2003)
Carinoma tremaphoros Thompson, 1900	JF293049	HQ856865	JF277713	JF277602	HQ848630	Andrade et al. (2012)
Cephalothrix bipunctata Bürger, 1892	KF935279	KF935335	KF935391	KF935447	KF935501	Kvist et al. (2014)
Cephalothrix filiformis (Johnston, 1828)	JF293054	HQ856842	JF277743	JF277594	HQ848616	Andrade et al. (2012)
Cephalothrix hongkongiensis Sundberg et al., 2003	JF293057	HQ856839	JF277739	JF277591	HQ848614	Andrade et al. (2012)
Cephalothrix rufifrons (Johnston, 1837)	—	HQ856841	JF277741	JF277592	HQ848604	Andrade et al. (2012)
Cephalothrix simula (Iwata, 1952)	—	AJ436891	AJ436988	AJ436836	AJ436945	Thollesson and Norenburg (2003)
Cephalothrix spiralis Coe, 1930	—	AJ436892	AJ436989	AJ436837	AJ436946	Thollesson and Norenburg (2003)
Tubulanus annulatus (Montagu, 1804)	JF293060	HQ856901	JF277717	JF277599	HQ848622	Andrade et al. (2012)
Tubulanus ezoensis Yamaoka, 1940	—	AB854620	—	—	—	present study
Tubulanus pellucidus (Coe, 1895)	JF293062	HQ856900	JF277708	JF277595	HQ848625	Andrade et al. (2012)
Tubulanus polymorphus Renier, 1804	JF293061	HQ856899	JF277716	JF277598	HQ848621	Andrade et al. (2012)
Tubulanus punctatus (Takakura, 1898)	JF293063	HQ856894	JF277748	JF277597	HQ848624	Andrade et al. (2012)
Tubulanus rhabdotus Corrêa, 1954	—	AJ436894	AJ436990	AJ436839	AJ436948	Thollesson and Norenburg (2003)
Tubulanus sexlineatus (Griffin, 1898)	JF293064	HQ856895	JF277747	JF277596	HQ848623	Andrade et al. (2012)
Tubulanus tamias sp. nov. (holotype)	LC042092	AB854621	LC042094	LC042091	LC042093	present study
Outgroup						
Novocrania anomala (Müller, 1776)	DQ279934[a]	DQ279949[a]	JF509710[b]	DQ280024[a]	—	[a]Giribet et al. (2006); [b]Andrade et al. (2012)
Terebratalia transversa (Sowerby, 1846)	JF509725	JF509729	JF509711	JF509720	JF509715	Andrade et al. (2012)

Table 3. Nucleotides showing polymorphism and their positions in the aligned 2252-base sequences of 28S rDNA from the holotype (AB854621 and AB854622) and the paratype (AB854623 and AB854624) of *Tubulanus tamias* sp. nov. Alignment of the four sequences were carried out by CLUSTAL W (Thompson et al., 1994) implemented in MEGA v.5.2.2 (Tamura et al., 2011).

Sequence	Site													
	558	639	705	706	1605	1851	1852	1853	1870	1871	1873	1874	1877	1878
AB854621 (holotype)	A	T	C	G	T	G	C	T	G	C	A	A	–	–
AB854622 (holotype)	A	T	–	–	T	G	C	T	A	A	C	G	A	A
AB854623 (paratype)	G	C	C	G	C	G	C	T	G	C	A	A	–	–
AB854624 (paratype)	G	C	C	G	C	–	–	–	G	C	A	A	–	–
Type of variation: i, intra-individual; s, intra-specific	s	s	i	i	s	i	i	i	i	i	i	i	i	i

657 nt (COI); the genes were concatenated for phylogenetic analyses by using MEGA ver. 5.2.2.

The ML analysis was conducted in RAxML ver. 8 (Stamatakis, 2014) under the GTR+G model; for 16S, 18S, and 28S, the data were partitioned by gene; for H3 and COI by codon position. Nodal support values were estimated by bootstrapping with 1000 pseudoreplicates. RAxML was called as follows (except the options for input and output file names, as well as the partition file name): raxmlHPC-PTHREADS-AVX -T 5 -f a -x 12345 -p 12345 -#1000 -m GTRGAMMA.

BI was conducted by using MrBayes ver. 3.2.4 (Ronquist and Huelsenbeck, 2003; Altekar et al., 2004), with two independent Metropolis-coupled analyses, each using four Markov chains of 10,000,000 generations. Trees were sampled every 100 generations. Run convergence was assessed by using Tracer ver. 1.6 (Rambaut et al., 2014). The equilibrium samples (after 25% of burn-in) were used to generate a 50% majority-rule consensus tree. For BI, jModeltest2 (Darriba et al., 2012) was used to determine the most suitable substitution model for each gene partition under the Bayesian information criterion, with the following settings: number of substitution schemes = 3; including models with equal/unequal base frequencies (+F); including models with/without a proportion of invariable sites (+I); including models with/without rate variation among sites (+G) (nCat = 4); optimized free parameters (K) = substitution parameters + 29 branch lengths + topology; base tree for likelihood calculations = ML tree; tree topology search operation = NNI. The optimal models were K80 + I + G for 18S; and GTR + I + G for 16S, 28S, H3, and COI.

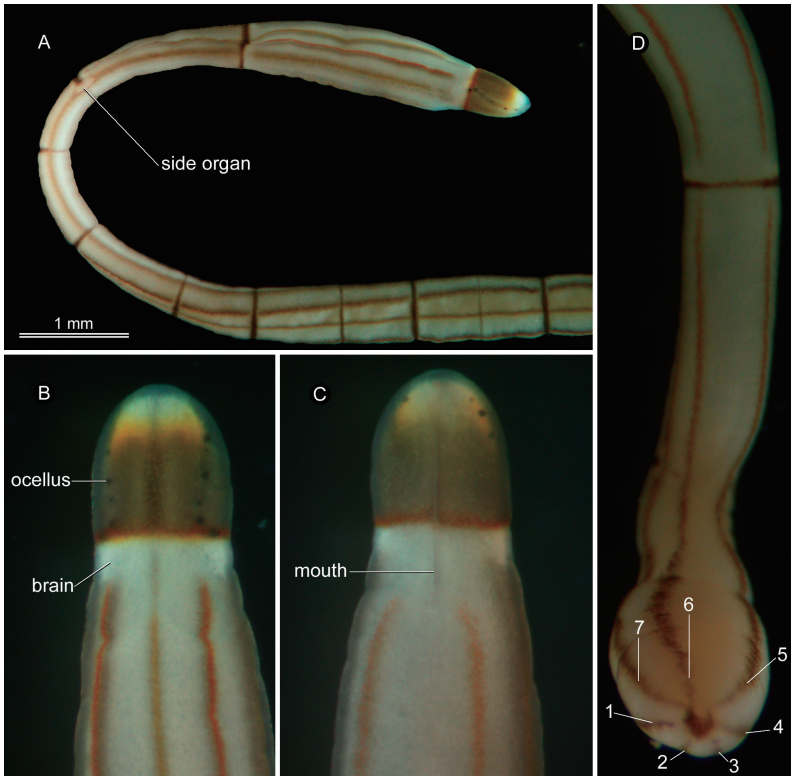

Fig. 1. *Tubulanus tamias* sp. nov., photographs of living specimens. **(A–C)** Paratype, ZIHU 4432. **(D)** Holotype, ZIHU 4430. **(A)** General appearance of the anterior end of the body fragment, showing the side organ. **(B)** Head, dorsal view. **(C)** Head, ventral view. **(D)** Posterior end of the body fragment, ventral view, showing the seven longitudinal stripes ("2" indicates the mid-dorsal stripe).

RESULTS

Taxonomy

Tubulanus tamias sp. nov.
(Figs. 1–6)

Material examined. Holotype, female, ZIHU 4430, serial transverse sections 9 μm thick, five slides. Allotype, male, ZIHU 4431, serial transverse sections, 14 μm thick, three slides. Paratype, sex unknown, ZIHU 4432, unsectioned anterior body fragment, preserved in 70% EtOH.

Description. *External features*. Paratype largest among three body fragments observed, measuring about 10 mm long, 0.6 mm in wide; holotype 8 mm long; allotype 5 mm long. Body white in basement color, decorated with numerous stripes and bands (Fig. 1A). Head demarcated from body, not wider than trunk, bluntly rounded anteriorly; white near anterior tip, posteriorly changing to olive color in a narrow, yellow transitional zone; with a dark olive mid-dorsal stripe. Black ocelli arranged in row on each side of head, from ventral margin near tip, postero-dorsally along lateral edge to dorso-lateral margin (Fig. 1B, C). Neck with dark orange ring completely encircling body; just posterior to neck ring, white mass visible in deeper portion of epidermis on both sides, corresponding to brain.

Body with seven olive-colored longitudinal stripes in deep epidermis, beginning close behind neck ring: three dorsal, single lateral on each side, and two ventral (Fig. 1D).

In shallower epidermis, narrow, light brown, longitudinal line runs above mid-dorsal olive stripe; dark orange longitudinal lines run above dorsal and ventral olive stripes on both sides.

Dark brown bands present at more or less regular intervals in posterior portion of body, alternating thick and thin. Body tends to constrict at thick bands when worm contracts. Side organs present at second band (Fig. 1A). The dark brown bands often interrupt the longitudinal stripes.

Body wall. Epidermal non-cellular inclusions absent. Epidermis of anterior body without intra-epithelial muscle fiber network. In brain region, thickness of epidermis/lateral body diameter > 0.1; *E* (*b*) = 0.11; *E* (*i*) = 0.06. Dermis forms distinct zone between epidermis and body-wall circular muscle layer (Fig. 2A). Thickness of dermis less than half of epidermal height (Fig. 2A). Muscle processes (or radial muscles) extend into epidermis in cephalic region (Fig. 2A). Muscles organized in outer circular and inner longitudinal layers; diagonal muscles not found; inner circular muscle layer present around rhynchocoel and alimentary canal (Fig. 2B). Muscle cross between body-wall outer circular muscle layer and these "inner" circular muscles not found. Longitudinal muscle plate poorly developed between rhynchocoel and foregut, but posteriorly conspicuous between rhynchocoel and intestine (Fig. 2C). Transverse muscle fibers present above mouth (Fig. 2D). Parenchyma barely distinguishable, except as membranes enclosing various body organ systems.

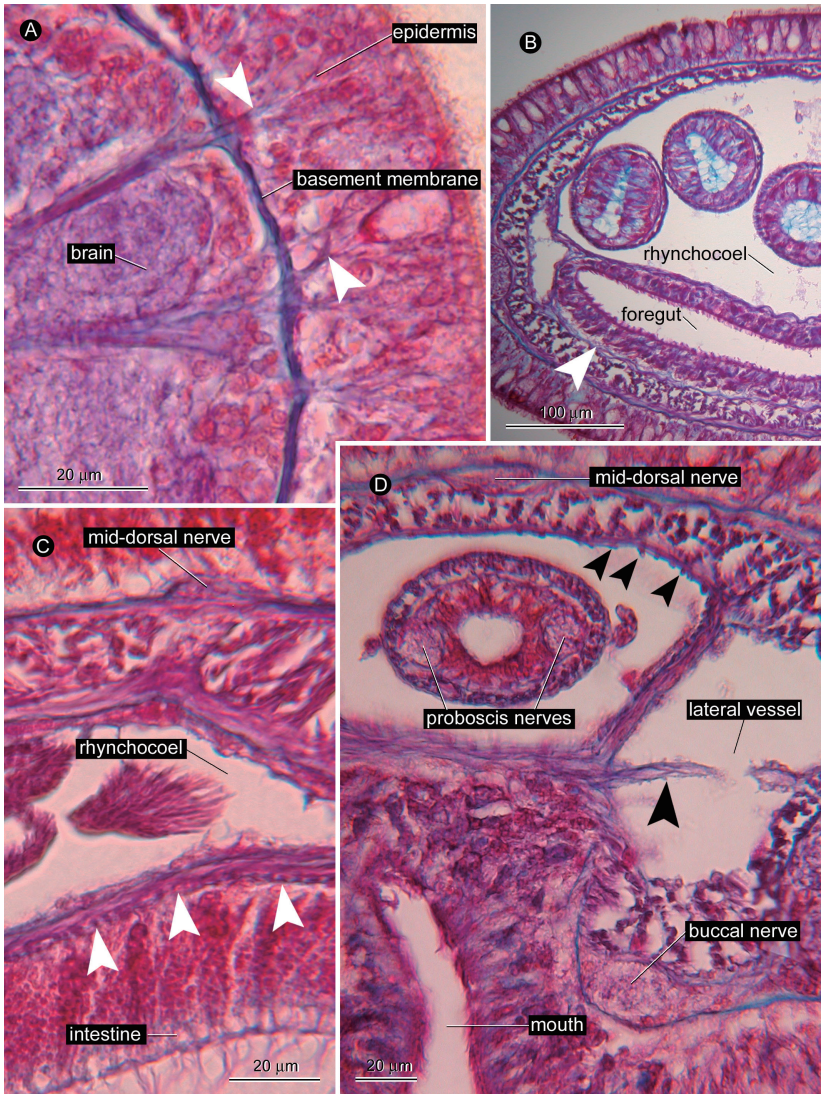

Fig. 2. *Tubulanus tamias* sp. nov., holotype, ZIHU 4430, photomicrographs of transverse sections. **(A)** Brain region, showing muscle processes in epidermis (arrowheads). **(B)** Foregut region, showing circular muscle around foregut (arrowhead). **(C)** Anterior intestinal region, showing longitudinal muscle plate (arrowheads). **(D)** Mouth region, showing transverse muscle fibers above mouth, penetrating lateral vessel (large arrowhead); small arrowheads indicate inner longitudinal muscles in the rhynchocoel wall.

Proboscis apparatus. Proboscis pore subterminal. Basophilic glandular cells present in rhynchodaeum (Fig. 3A). Rhynchocoel musculature consists of circular muscles, except in brain region, where inner longitudinal muscles also present (Fig. 2D); circular muscle layer not extremely thick posteriorly, but posterior rhynchocoel chamber (about 1 mm in length) present (Fig. 3B–H). Rhynchocoel not reaching hind end of body. Proboscis composed of three regions (anterior, middle, and posterior, in retracted state). Anterior region short (about 500 µm long), with epithelium largely consisting of acidophilic components (Figs. 2D, 4A), two proboscis nerves, circular muscle layer, longitudinal muscle layer, and thin endothelium; posteriorly increasing basophilic glandular cells in epithelium, gradually leading to main, middle region. Middle region with bilaterally symmetrical epithelium (Fig. 4B), two proboscis nerves, circular and longitudinal muscle layers, and delicate endothelium; epithelium consists predominantly of basophilic glandular cells, thicker laterally, thinner dorsally and ventrally; thin epithelium wider dorsally than ventrally, resulting in proboscis lumen (in retracted state) shaped like golf tee or narrowly pleated mushroom. Posterior region short, with epithelium containing acidophilic cells; proboscis nerves and circular muscles inconspicuous in light microscopy; with longitudinal muscles and thin endothelium (Fig. 4C); posteriorly leading to proboscis retractor muscle (Fig. 3B). Pseudocnidae or proboscis armature not found.

Alimentary system. Mouth opens just behind brain. Esophagus absent. Stomach histologically not differentiated; gradually leading to intestine. Intestinal cecum absent. Intestinal diverticula absent. Intestine with sphincters (Fig. 4D), up to 30 µm thick, probably corresponding to position of epidermal constrictions arranged at regular intervals.

Circulatory system. Cephalic vasculature, forming blood lacunae in front of cerebral ganglia, consists of single main channel abutting rhynchodaeum on each side, sparsely connected by dorsal commissures; main blood lacunar channel ventrally connected to each other just behind proboscis

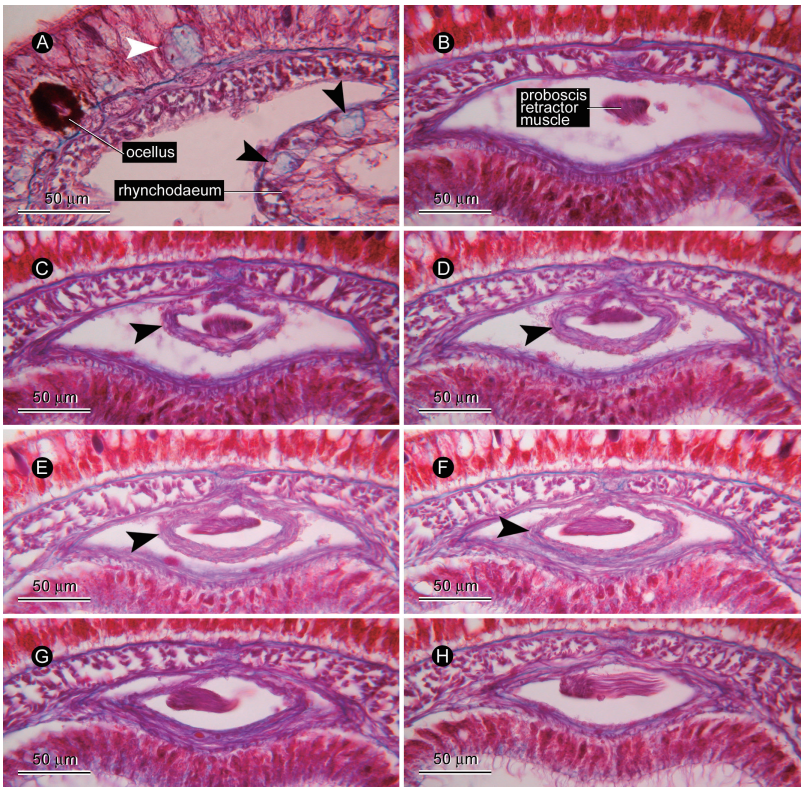

Fig. 3. *Tubulanus tamias* sp. nov., holotype, ZIHU 4430, photomicrographs of transverse sections. **(A)** Precerebral region showing basophilic glandular cells in rhynchodaeum (black arrowheads) and basal portion of epidermis (white arrowhead). **(B–H)** Serial sections of the region near nephridiopore and side organ, showing anterior tip of posterior rhynchocoel chamber (arrowheads).

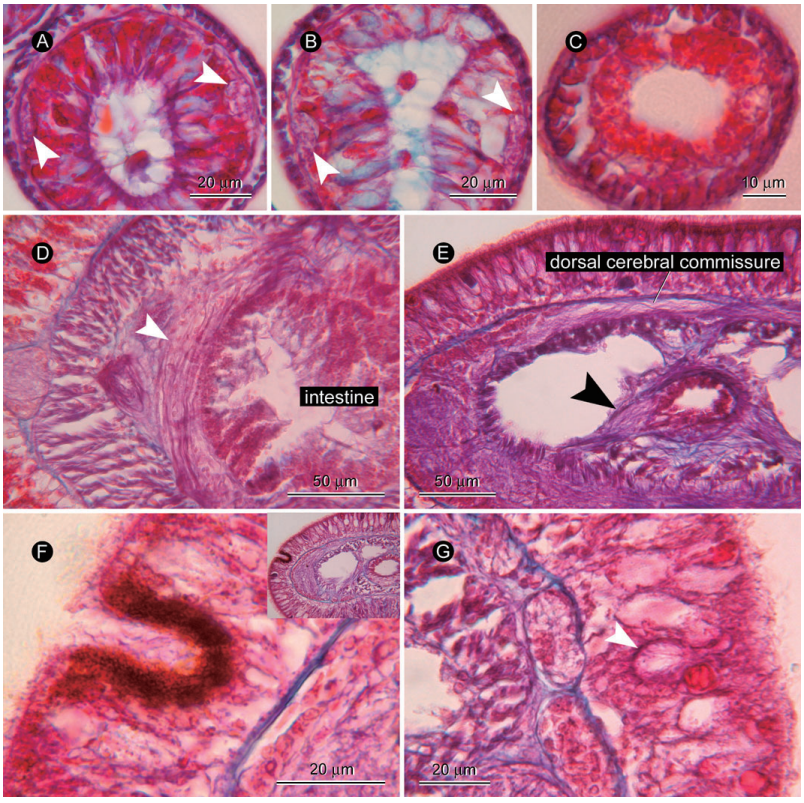

insertion, forming U-shape in cross section; posteriorly, U-shaped lacuna immediately branches to lateral vessel on each side just anterior to mouth; in brain region, transverse muscle fiber bundle frequently penetrates lateral vessel (Fig. 2D); each lateral vessel extends further backward and abuts rhynchocoel and alimentary canal. No muscle fibers found lateral-to-lateral vessel in light microscopy. Mid-dorsal vessel, vascular plexus in foregut region, and rhynchocoelic blood vessel all absent.

Nervous system. Cerebral ganglia and lateral nerve cords situated between epidermal basement membrane and body-wall outer circular muscle layer. Single dorsal cerebral commissure (Fig. 4E), about 10 µm thick; ventral cerebral commissure 40 µm thick. Pair of nerve bundles (about 12 µm thick) extend medioanteriorly from anterior surface of ventral ganglia (Fig. 4E), running along proboscis insertion, eventually reaching proboscis nerves. Cerebral ganglia with distinct outer neurilemma, but no inner neurilemma. No statocyst in brain. Four large nerves in head region absent. Single mid-dorsal nerve extends from dorsal cerebral commissure, running posteriorly between epidermal basement membrane and body-wall outer circular muscle layer; occasionally extends nerve fibers innervating rhynchocoel wall. Posterior junction of lateral nerve cords unknown. No neurochord cells in brain or lateral nerve cords. Myofibrillae not found in lateral nerve cords. Pair of buccal nerves present (Fig. 2D).

Sensory system. Nine to 10 pairs of epidermal pigment-cup ocelli present on both sides of head anterior to cerebral organs. Two types of eyes: anterior eight to nine pairs of eyes abut connective tissue of basement membrane proximally (Fig. 3A), each containing bundle of rod-shaped structures (up to seven per eye cup) (Fig. 5); the posterior-most pair of eyes situated near brain, distally within epidermis, with cavity of pigment cup densely ciliated and reaching exterior (Fig. 4F). Apical organ absent. Typical basophilic glands absent, but numerous basophilic glandular cells aggregated in basal portion of epidermis and rhyn-

Fig. 4. *Tubulanus tamias* sp. nov., holotype, ZIHU 4430, photomicrographs of transverse sections. **(A)** Anterior portion of proboscis with two nerves (arrowheads). **(B)** Middle main portion of proboscis with two nerves (arrowheads). **(C)** Posterior portion of proboscis. **(D)** Intestinal sphincter (arrowhead). **(E)** Brain region, showing origin of proboscis nerves (arrowhead). **(F)** Epidermal eye. **(G)** Ciliated canal in epidermis (arrowhead).

chodaeal epithelium (Fig. 3A). Cerebral sensory organ represented by short ciliated canal in epidermis closely behind brain (Fig. 4G). Side organ present on each side (Fig. 6A), just behind nephridiopore.

Excretory system. Excretory collecting tubule extends from middle stomach region to stomach–intestine junction, occasionally branched (or convoluted) (Fig. 6B), terminating in single nephridiopore on each side (Fig. 6C). No circular muscles found lateral to excretory canal. Nephridial gland absent. Glandular components in excretory tubules absent.

Reproductive system. Sexes separate. Single gonad situated dorsolaterally to intestine, arranged in row on each side. Testis simple, not bilobed (Fig. 6D). Gonoduct situated dorsally (Fig. 6E).

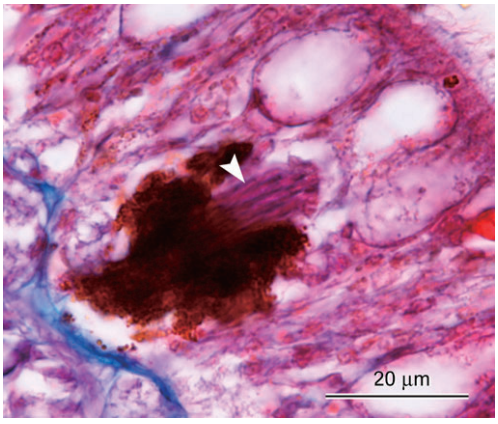

Fig. 5. *Tubulanus tamias* sp. nov., holotype, ZIHU 4430, photomicrograph of transverse section through epidermal ocellus, showing bundle of rod-shaped structures in the eye cup (arrowhead).

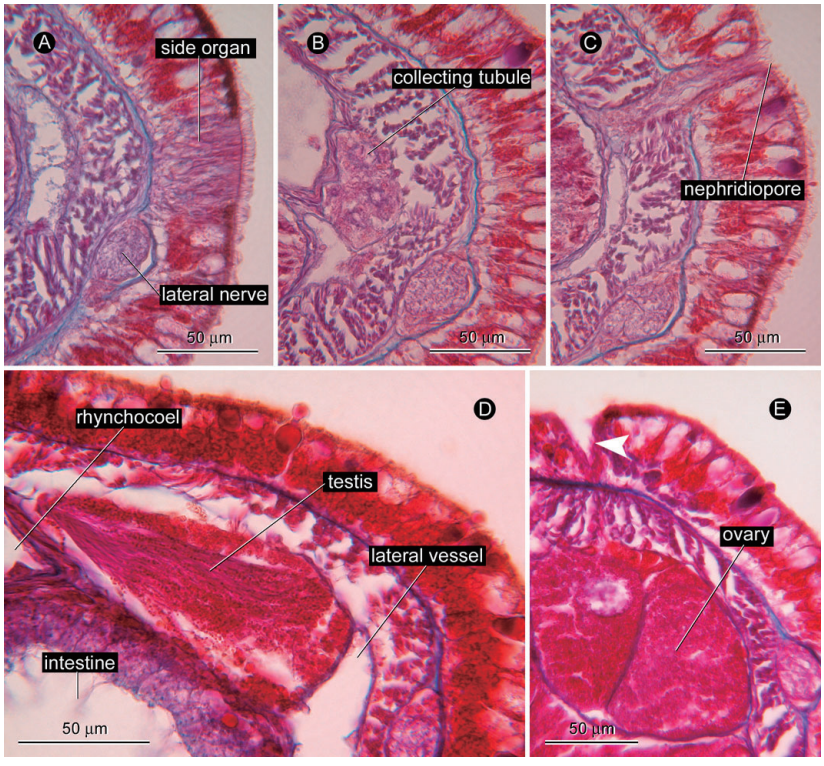

Fig. 6. *Tubulanus tamias* sp. nov., photomicrographs of transverse sections. **(A–C, E)** Holotype, ZIHU 4430. **(D)** Allotype, ZIHU 4431. **(A)** Side organ. **(B)** Excretory collecting tubule. **(C)** Nephridiopore. **(D)** Testis. **(E)** Gonopore opening dorsally (arrowhead).

Etymology. The specific name is a noun in the nominative singular, after the name of the chipmunks genus, *Tamias* Illiger, 1811 (Rodentia: Sciuridae), alluding to the characteristic longitudinal stripes on the body.

Remarks. *Tubulanus tamias* sp. nov. differs from its 34 congeners in body coloration and markings (Table S2). Only *T. rhabdotus* Corrêa, 1954 and *T. frenatus* (Coe, 1904) are similar to *T. tamias* in having a pale basement body color with both longitudinal and transverse dark markings. *Tubulanus tamias* has seven stripes (three dorsal, a single lateral on each side, and two ventral), whereas *T. frenatus* has three (mid-dorsal and lateral) stripes and *T. rhabdotus* has only two (lateral). The pattern of stripes and rings is similar between *T. tamias* and *T. cingulatus* (Coe, 1904), but the ground color is pale and markings are dark in *T. tamias*, while the converse is the case in *T. cingulatus*.

Tubulanus roretzi Senz, 1997 was described based on fixed material collected in Japanese waters (details about the locality and habitat are not known). Body coloration in the living state in this species is thus unknown. In internal anatomy, however, *T. roretzi* clearly differs from *T. tamias* because it has (1) a complete body-wall inner circular muscle layer (vs incomplete in *T. tamias*), (2) muscle crosses between the body-wall inner and outer circular muscle layers both dorsally and ventrally (vs absent in *T. tamias*), and (3) rhynchocoel vessels (vs absent in *T. tamias*).

28S rDNA polymorphism

Two different haplotypes were detected in each of the holotype and one paratype for which sequences were determined (Table 3). Among the aligned 2252-base sequences, there were 14 variable sites, of which three varied only between the individuals, and 11 varied within and between the individuals. In the holotype, this intra-individual variation was found at positions 705 and 706, and between 1870 and 1878 (the 5′ end of the aligned sequences is site 558 in Table 3), corresponding to the D2 and D7 regions (Gillespie et al., 2006), respectively. In the paratype, intra-individual variation occurred at positions 1851 to 1853 (D7 region).

Molecular phylogeny

Topologically, the resulting ML tree (Fig. 7, ln L = –23771.502465) and BI tree (Fig. S1) were exactly the same, with *T. tamias* appearing as sister to a well-supported clade (100% bootstrap value [BS], and 1.00 posterior probability [PP]) formed by *T. punctatus*, *T. sexlineatus* (Griffin, 1898), and *T. rhabdotus*. The clade formed by *T. tamias*, *T. punctatus*, *T. sexlineatus*, and *T. rhabdotus* (with 99% BS and 1.00 PP) was sister to a poorly supported clade that includes *Carinina plecta* Kajihara, 2006, *Callinera grandis* Bergendal, 1903, and *Tubulanus pellucidus* (Coe, 1895),

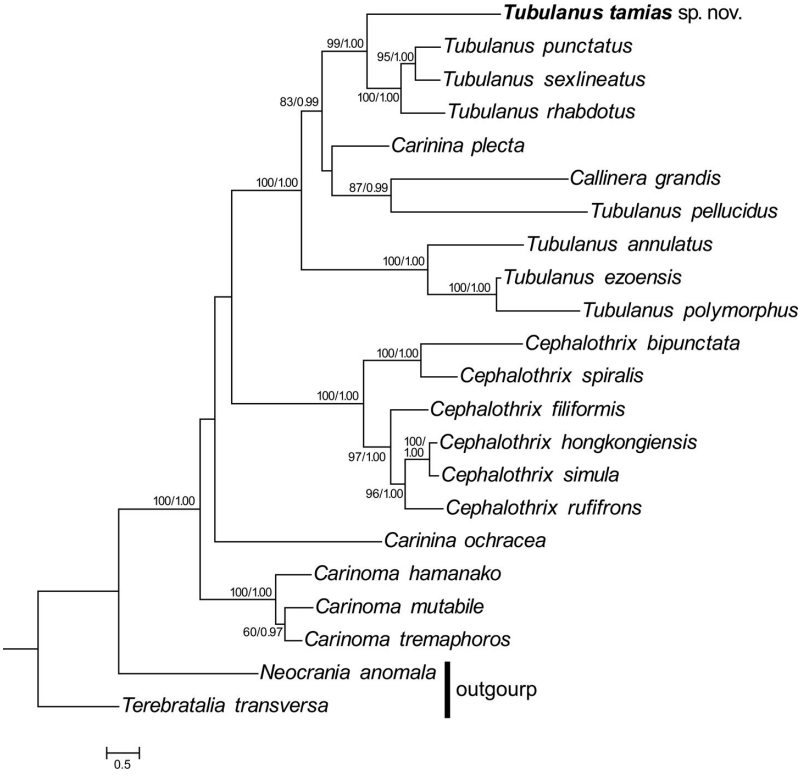

Fig. 7. Phylogeny resulting from a maximum-likelihood analysis (ln *L* = –23771.502465). Numbers near nodes indicate bootstrap support values (≥ 60%) and posterior probability in Bayesian analysis (≥ 0.95).

with the latter two being sister to each other (87% BS, 0.99 PP). These tubulanids formed a clade supported with 83% BS and 0.99 PP, which was sister to a strongly supported clade (100% BS, 1.00 PP) comprised of *T. annulatus* (Montagu, 1804), *T. ezoensis*, and *T. polymorphus* Renier, 1804. While these tubulanids formed a well-supported clade (100% BS, 1.00 PP), our results thus indicate that the genus *Tubulanus* is non-monophyletic.

The six species of *Cephalothrix* included in the present analyses formed a monophyletic group (100% BS, 1.00 PP), which was sister to the aforementioned tubulanids, while the support values for the clade containing these two groups were low. This clade turned out to be sister to the tubulanid *Carinina ochracea* Sundberg et al., 2009, although its branch support was not significant. Our analyses thus failed to resolve the phylogenetic position of *C. ochracea*, but suggested that the family Tubulanidae is unlikely to be monophyletic.

DISCUSSION

28S rDNA polymorphism

To our knowledge, this study is the first to report intra-individual polymorphism in 28S rDNA in the Metazoa, although Carranza et al. (1996) demonstrated such polymorphism in the 18S rDNA gene in a tricladid flatworm and attributed this to incomplete concerted evolution. Concerted evolution of repetitive DNA sequences homogenizes multiple copies of ribosomal genes in the genome so that they are identical (Elder and Turner, 1995; Liao, 1999). Sonnenberg et al. (2007) analysed 230 fragments of the D1–D2 region of 28S rDNA among 158 species of animals belonging to Annelida, Mollusca, Arthropoda, Nematoda, and Chordata, and observed 15 fragments with a single ambiguous position, six fragments with two such positions, and four with three ambiguities. Sonnenberg et al. (2007) concluded that, on average, far fewer than 0.1% of the sequence positions surveyed were polymorphic but did not confirm actual intra-individual polymorphism by means such as molecular cloning. We cannot explain the incomplete concerted evolution observed in *T. tamias*, but if the tandem repeat units of the nuclear rDNA complex were located on two different chromosomes in this organism, this might have contributed to the intra-individual polymorphism.

Two different types of ocelli

Eyes are rare in palaeonemerteans. Among ~110 valid species in Palaeonemertea s. str., only the following six have been reported to have eyes: *Cephalotrichella signata* (Hubrecht, 1879) (Wijnhoff, 1913); *Carinesta tubulanoides* Gibson, 1990; *Cephalotrichella alba* Gibson and Sundberg, 1992; *Balionemertes australiensis* Sundberg et al., 2003; *Hubrechtia desiderata* (Kennel, 1891) (Bürger, 1895); and *Tubulanus riceae* Ritger and Norenburg, 2006 (summarized in Chernyshev, 2011). The adult ocelli so far known in palaeonemerteans are pigment-cup type, embedded in epidermis, basally abutting the basement membrane (Wijnhoff, 1913; Gibson, 1990; Gibson and Sundberg, 1992; Sundberg et al., 2003; Ritger and Norenburg, 2006); however, previous literature does not mention about the structure of the photoreceptor in the optical cavity, thus it has been unknown whether it is of ciliated or rhabdomeric type. Döhren et al. (pers. comm.) however have recently found in TEM observations that the eyes in some palaeonemertean planuliform larvae are situated in the epidermis and composed of ciliated photoreceptor cells, although provisional eyes have never been reported in larvae of *Tubulanus* (Iwata, 1960; Norenburg and Stricker, 2002; Chernyshev, 2011).

In the present study, we illustrated that *T. tamias* possesses nine to ten pairs of epidermal, pigment-cup eyes, (1) the anterior eight to nine pairs of which are located in the base of the epidermis, resting upon the basement membrane, with the optical cavity containing numerous, rod-shaped structures that resemble rhabdomeric photoreceptor cells (Fig. 5), and that (2) the posterior-most pair are situated near the surface of the epidermis, with the optical cavity opening to the exterior and filled with cilia (Fig. 4F). We speculate that (1) the anterior eyes are formed additively from posterior to anterior in the post-planuliform stage, and (2) the posterior-most pair are remnants of planuliform larval eyes, taking into account the evidences that (1) overall, the eyes become progressively smaller from posterior to anterior, and (2) some of the epidermal eyes in palaeonemertean planuliform larvae with ciliated photoreceptor cells have

optical cavities that are open to the exterior (Döhren et al., pers. comm.). In some other spiralian taxa, the larval eyes (with ciliary photoreceptors in some cases) precede adult eyes (with rhabdomeric photoreceptors), either degenerating or persisting to be modified into adult eyes; those kinds of transitions are known in Annelida (Holborow and Laverack, 1972; Eakin and Hermans, 1988; Bartolomaeus, 1992a, 1993; Blumer, 1997; Arendt et al., 2004) and Mollusca (Salvini-Plawen, 1980, 1982; Bartolomaeus, 1992b; Blumer, 1996, 1998). The posterior-most pair of eyes in the adult *Tubulanus tamias* may also undergo such modification of larval eyes.

On the other hand, we cannot rule out the possibility that the posterior-most eyes in *T. tamias* may represent eyes of juvenile (instead of larval) stage, as Döhren and Bartolomaeus (2007) reported that in the heteronemertean *Lineus viridis* (Müller, 1774), the adult eyes are rhabdomeric, while the juvenile ones are ciliary. That no larva in *Tubulanus* has been reported to have eyes (Iwata, 1960; Norenburg and Stricker, 2002; Chernyshev, 2011) may come in favor of the possibility in which the posterior-most eyes in *T. tamias* are actually the juvenile eyes, instead of larval ones.

Non-monophyly of *Tubulanus* and Tubulanidae

As has been already indicated in Andrade et al. (2012) and Kvist et al. (2014), the genus *Tubulanus* is likely to be paraphyletic with respect to *Callinera*. In this paper, we could have established a new genus for the clade comprised of *T. punctatus*, *T. rhabdotus*, *T sexlineatus*, and *T. tamias*, and transferred *T. pellucidus* to *Callinera*, thereby made the name *Tubulanus* applied only to the clade containing its type species *T. polymorphus*. As the time being, however, we leave the systematic revision of Tubulanidae to future studies with expanded taxon sampling, placing our new species in *Tubulanus*, since it perfectly matches the traditional taxon concept of the genus.

ACKNOWLEDGMENTS

We thank Mrs. Junko Sato for help in histological preparation and photomicrography; the staff at the Amakusa Marine Biological Laboratory, Kyushu University, for making available research facilities; Ikumasa Ganaha for help in molecular work; and Professor Matthew H. Dick for critical comments. This study was financially supported by a Narishige Zoological Science Award in FY2009 to HK.

REFERENCES

Altekar G, Dwarkadas S, Huelsenbeck JP, Ronquist F (2004) Parallel Metropolis-coupled Markov chain Monte Carlo for Bayesian phylogenetic inference. Bioinformatics 20: 407–415

Andrade SCS, Strand M, Schwartz M, Chen H, Kajihara H, Döhren Jv, et al. (2012) Disentangling ribbon worm relationships: multilocus analysis supports traditional classification of the phylum Nemertea. Cladistics 28: 141–159

Arendt D, Tessmar-Raible K, Snyman H, Dorresteijn A, Wittbrodt J (2004) Ciliary photoreceptors with a vertebrate-type opsin in an invertebrate brain. Science 306: 869–871

Bartolomaeus T (1992a) Ultrastructure of the photoreceptors in certain larvae of the Annelida. Microfauna Mar 7: 191–214

Bartolomaeus T (1992b) Ultrastructure of the photoreceptors in the larvae of *Lepidochiton cinereus* (Mollusca, Polyplacophora) and *Lacuna divaricata* (Mollusca, Gastropoda). Microfauna Mar 7: 215–236

Bartolomaeus T (1993) Different photoreceptors in juvenile *Ophelia rathkei* (Annelida, Opheliida). Microfauna Mar 8: 99–114

Bergendal D (1903) Till kännedomen om de nordiska Nemertinerna. 4. Förteckning öfver vid Sveriges vestkust iakttagna Nemertiner. Ark Zool 1: 85–156

Blumer MJF (1996) Alterations of the eyes during ontogenesis in *Aporrhais pespelecani* (Mollusca, Caenogastropoda). Zoomorphology 116: 121–131

Blumer MJF (1997) The larval ocelli of *Golfingia misakiana* (Sipuncula, Golfingiidae) and of a pelagosphera of another unidentified species. Zoomorphology 117: 115–120

Blumer MJF (1998) Alterations of the eyes of *Carinaria lamarcki* (Gastropoda, Heteropoda) during the long pelagic cycle. Zoomorphology 118: 183–194

Bürger O (1892) Zur Systematik der Nemertinenfauna des Golfs von Neapel. Nachr Königl Ges Wiss Georg-Augusts-Univ 5: 137–178

Bürger O (1895) Die Nemertinen des Golfes von Neapel und der angrenzenden Meeres-Abschnitte. F F Golf Neapel 22: 1–743

Carranza S, Giribet G, Ribera C, Baguñà J, Riutort M (1996) Evidence that two types of 18S rDNA coexist in the genome of *Dugesia* (*Schmidtea*) *mediterranea* (Platyhelminthes, Turbellaria, Tricladida). Mol Biol Evol 13: 824–832

Chernyshev AV (2011) Comparative Morphology, Systematics and Phylogeny of the Nemerteans. Dalnauka, Vladivostok [in Russian]

Coe WR (1895) Descriptions of three new species of New England palaeonemerteans. Trans Connecticut Acad Art Sci 9: 515–522

Coe WR (1901) Papers from the Harriman Alaska Expedition. XX. The nemerteans. Proc Wash Acad Sci 3: 1–84

Coe WR (1904) Nemerteans of the Pacific Coast of North America. Part II. Harriman Alaska Ser 11: 111–220

Coe WR (1930) Two new species of nemerteans belonging to the family Cephalotrichidae. Zool Anz 89: 97–103

Corrêa DD (1954) Nemertinos do litoral brasileiro. Bol Fac Fil Ciênc Letr Univ São Paulo 19: 1–90

Criscuolo A, Gribaldo S (2010) BMGE (block mapping and gathering with entropy): selection of phylogenetic informative regions from multiple sequence alignments. BMC Evol Biol 10: 210

Darriba D, Taboada GL, Doallo R, Posada D (2012) jModelTest2: more models, new heuristics and parallel computing. Nat Methods 9: 772

Döhren Jv, Bartolomaeus T (2007) Ultrastructure and development of the rhabdomeric eyes in *Lineus viridis* (Heteronemertea, Nemertea). Zoology 110: 430–438

Eakin RM, Hermans CO (1988) Eyes. In "The Ultrastructure of the Polychaeta", Ed by W Westheide, CO Hermans, Microfauna Mar 4: 135–156

Edgar RC (2004) MUSCLE: a multiple sequence alignmnet method with reduced time and space complexity. BMC Bioinfomatics 5: 113

Elder JF, Turner BJ (1995) Concerted evolution of repetitive DNA sequences in eukaryotes. Q Rev Biol 70: 297–320

Fernández-Álvarez FÁ, Anadón N (2013) Redescription of *Tubulanus mawsoni* (Wheeler 1940) comb. nov. (Palaeonemertea: Tubulanidae) from the Bellingshausen Sea (Antarctica). NZ J Zool 40: 263–279

Gibson R (1990) The macrobenthic nemertean fauna of Hong Kong. In "The Marine Flora and Fauna of Hong Kong and Southern China II, Vol 1, Introduction and Taxonomy" Ed by B Morton, Hong Kong University Press, Hong Kong, pp 33–212

Gibson R (1994) Nemerteans. Field Studies Council, Shrewsbury

Gibson R (2014) *Tubulanus*. In "World Nemertea Database" Ed by Norenburg J, Gibson R. Accessed through: World Register of Marine Species at http://www.marinespecies.org/aphia.php?p=taxdetails&id=122388 on 1 November 2014

Gibson R, Sundberg P (1992) Three new nemerteans from Hong Kong. In "The Marine Flora and Fauna of Hong Kong and

Southern China III, Vol 1" Ed by B Morton, Hong Kong University Press, Hong Kong, pp 97–129
Gillespie JJ, Johnston JS, Cannone JJ, Gutell RR (2006) Characteristics of the nuclear (18S, 5.8S, 28S and 5S) and mitochondrial (12S and 16S) rRNA genes of *Apis mellifera* (Insecta: Hymenoptera): structure, organization, and retrotransposable elements. Insect Mol Biol 15: 657–686
Giribet G, Okusu A, Lindgren AR, Huff SW, Schrödl M, Nishiguchi MK (2006) Evidence for a clade composed of molluscs with serially repeated structures: Monoplacophorans are related to chitons. Proc Natl Acad Sci USA 103: 7723–7728
Griffin BB (1898) Description of some marine nemerteans of Puget Sound and Alaska. Ann NY Acad Sci 11: 193–217
Holborow PL, Laverack MS (1972) Presumptive photoreceptor structures of the trochophore of *Harmothoe imbricata* (Polychaeta). Mar Behav Physiol 1: 139–156
Hubrecht AAW (1879) The genera of European nemerteans critically revised, with description of several new species. Notes Leyden Mus 1: 193–232
Illiger C (1811) Prodromus Systematis Mammalium et Avium. C Salfeld, Berlin
Iwata F (1952) Nemertini from the coasts of Kyusyu. J Fac Sci Hokkaido Univ Ser 6 Zool 11: 126–148
Iwata F (1960) Studies on the comparative embryology of the nemerteans with special reference to their inter-relationships. Publ Akkeshi Mar Biol Stn 10: 1–51
Johnston G (1828) Contributions to the British fauna. Zool J 4: 52–57
Johnston G (1837) Miscellanea zoologica. II. A description of some planarian worms. Mag Zool Bot 1: 529–538
Kajihara H (2006) Four palaeonemerteans (Nemertea: Anopla) from a tidal flat in middle Honshu, Japan. Zootaxa 1163: 1–47
Kajihara H (2007) A taxonomic catalogue of Japanese nemerteans (Phylum Nemertea) Zool Sci 24: 287–326
Kajihara H, Yamasaki H, Andrade SCS (2011) *Carinoma hamanako* sp. nov. (Nemertea: Palaeonemertea), the first representative of the genus from the Northwest Pacific. Spec Div 16: 149–165
Kennel Jv (1891) Über einige Nemertinen. Sber Naturf Ges Dorpat 9: 289–293
Kim C-G, Zhou H-Z, Imura Y, Tominaga O, Su Z-H, Osawa S (2000) Pattern of morphological diversification in the *Leptocarabus* ground beetles (Coleoptera: Carabidae) as deduced from mitochondrial ND5 gene and nuclear 28S rRNA sequences. Mol Biol Evol 17: 137–145
Kvist S, Laumer CE, Junoy J, Giribet G (2014) New insights into the phylogeny, systematics and DNA barcoding of Nemertea. Invertebr Syst 28: 287–308
Liao D (1999) Concerted evolution: molecular mechanism and biological implications. Am J Hum Gen 64: 24–30
Luan Y-X, Mallatt JM, Xie R-D, Yang Y-M, Yin W-Y (2005) The phylogenetic positions of three basal-hexapod group (Protura, Diplura, and Collembola) based on ribosomal RNA gene sequences. Mol Biol Evol 22: 1579–1592
Montagu G (1804) Description of several marine animals found on the south coast of Devonshire. Trans Linn Soc Lond 7: 61–85
Müller OF (1774) Vermium terrestrium et fluviatilium, seu animalium infusoriorum, helminthicorum et testaceorum, non marinorum, succincta historia, Vol. 1, Part 2. Heineck & Faber, Copenhagen and Leipzig
Müller OF (1776) Zoologiae Danicae prodromus seu animalium Daniae et Norvegiae indigenarum characteres, nomina, et synonyma imprimis popularium. Hallager, Copenhagen
Norenburg JL, Stricker SA (2002) Phylum Nemertea. In "Atlas of Marine Invertebrate Larvae" Ed by Young CM, Academic Press, San Diego, pp 163–177
Rambaut A, Suchard MA, Xie W, Drummond AJ (2014) Tracer v 1.6, available at http://beast.bio.ed.ac.uk/Tracer
Renier SA (1804) Prospetto della Classe dei Vermi. Padua, pp xv–xxvii
Ritger RK, Norenburg JL (2006) *Tubulanus riceae* new species (Nemertea: Anopla: Palaeonemertea: Tubulanidae), from South Florida, Belize and Panama. J Nat Hist 40: 931–942
Ronquist F, Huelsenbeck JP (2003) MrBayes 3: Bayesian phylogenetic inference under mixed models. Bioinformatics 19: 1572–1574
Salvini-Plawen Lv (1980) Was ist eine Trochophora? Eine Analyse der Larventypen mariner Protostomier. Zool Jahrb Anat Ontog 103: 389–423
Salvini-Plawen Lv (1982) On the polyphyletic origin of photoreceptors. In "Visual Cells in Evolution" Ed by JA Westfall, Raven, New York, pp 137–154
Senz W (1997) Morphologie und klassifikatorische Position einiger anopler Nemertinen (Nemertini: Anopla). Ann Naturh Mus Wien 99B: 423–496
Sonnenberg R, Nolte AW, Tautz D (2007) An evaluation of LSU rDNA D1–D2 sequences for their use in species identification. Front Zool 4: 6
Sowerby G (1846) Descriptions of Tertiary fossil shells from South America. As an appendix to "Geological observations on South America" by C Darwin, Smith, Elder & Co., London, pp 249–264
Stamatakis A (2014) RAxML version 8: a tool for phylogenetic analysis and post-analysis of large phylogenies. Bioinformatics 30: 1312–1313
Sundberg P, Gibson R, Olsson U (2003) Phylogenetic analysis of a group of palaeonemerteans (Nemertea) including two new species from Queensland and the Great Barrier Reef, Australia. Zool Scr 32: 279–296
Sundberg P, Chernyshev AV, Kajihara H, Kånneby T, Strand M (2009) Character-matrix based descriptions of two new nemertean (Nemertea) species. Zool J Linn Soc 157: 264–294
Takakura U (1898) Misaki kinbôsan himomushirui (Nemertine) no bunrui [A classification of the nemerteans of the Misaki region]. Zool Mag 10: 38–44, 116–120, 184–187, 331–337, 424–429 [in Japanese]
Tamura K, Peterson D, Peterson N, Stecher G, Nei M, Kumar S (2011) MEGA5: molecular evolutionary genetics analysis using maximum likelihood, evolutionary distance, and maximum parsimony methods. Mol Biol Evol 28: 2731–2739
Thollesson M, Norenburg JL (2003) Ribbon worm relationships: a phylogeny of the phylum Nemertea. Proc Roy Soc B 270: 407–415
Thompson CB (1900) *Carinoma tremaphoros*, a new mesonemertean species. Zool Anz 23: 627–630
Thompson JD, Higgins DG, Gibson TJ (1994) CLUSTAL W: improving the sensitivity of progressive multiple sequence alignment through sequence weighting, position-specific gap penalties and weight matrix choice. Nucleic Acids Res 22: 4673–4680
Wijnhoff G (1913) Die Gattung *Cephalothrix* und ihre Bedeutung für die Systematik der Nemertinen. II. Systematischer Teil. Zool Jb Abt Syst Ökol Geogr Tiere 34: 291–320
Yamaoka T (1940) The fauna of Akkeshi Bay. IX. Nemertini. J Fac Sci Hokkaido Imp Univ Ser VI Zool 7: 205–263
Yamasaki H, Hiruta SF, Kajihara H (2013) Molecular phylogeny of kinorhynchs. Mol Phylogenet Evol 67: 303–310

(Received November 4, 2014 / Accepted April 6, 2015)